Universitat de Barcelona

SPECTRAL FEATURES OF S0 GALAXIES IN LOW- AND HIGH-DENSITY ENVIRONMENTS

Author: José Luis Tous Mayol

Facultat de Física, Universitat de Barcelona, Diagonal 645, 08028 Barcelona, Spain

Advisor: Josep Maria Solanes Majúa

Barcelona, June 2018

Contents

ABSTRACT

We aim to investigate the possibility that the formation pathway of lenticular galaxies depends on the environment, using their spectra. To this end, we estimate extinction-corrected local densities for all the galaxies with $z \lesssim 0.1$ in the Sloan Digital Sky Survey Data Release 12 within the limits of the Legacy Survey. The local densities are cross-matched with two morphological catalogues, one in which galaxies are visually classified by Nair and Abraham (2010), and one in which morphologies are assigned by a neural network based classification by Domínguez Sánchez et al. (2018), in order to compile subsets of lenticular galaxies in low- and high-density environments. We also compute the mean spectra representative of each one of the datasets by stacking the normalized, rest-frame shifted individual spectra. The effects of inclination biases and morphological misclassifications in these composite spectra are discussed. We find that lenticular galaxies in low-density regions are generally bluer with enhanced emission lines in comparison with their high-density counterparts. The comparative also reveals a possible excess of automatically classified S0 galaxies in low-density regions with a relevant reservoir of ionized gas and star formation activity, which may indicate contamination from Sa. In visually classified galaxies the misclassification errors involve both Sa and E and tend to be more important in galaxies with intermediate ($30^{\rm o} < i < 60^{\rm o}$) inclinations.

I. INTRODUCTION

It was in 1936 that Hubble introduced for the first time a hypothetical class of S0 galaxies which were supposed to have characteristics intermediate between those of ellipticals (E) and spirals (S). Subsequent work by Hubble himself and other eminent morphologists such as Sandage (1961) suggested that the lenticular galaxies, which occur in large numbers in rich clusters, were to be identified as these S0 galaxies postulated by Hubble. This classification appeared to be reasonable because lenticulars contain a significant spheroidal central-bulge component and a disk component. Although these two components are present, to a greater or lesser extent, in most spirals (the exception being some bulgeless late-type spirals) the main difference between them and lenticulars is that the later class of objects host smooth disks devoid of spiral structure and that contain little or no interstellar gas and dust.

The observation that lenticulars comprise the dominant population in the central regions of many rich clusters of galaxies led Spitzer and Baade (1951) to suggest that such objects were, in fact, spirals from which the gas has been removed by collisions between galaxies. About twenty years latter Gunn and Gott (1972) showed that it is much more probable that the gas in cluster S0 is removed by the ram pressure produced by the intracluster medium upon the disks as cluster galaxies move through it. The explanation is that, in the simple case when the relative velocity is normal to the surface and momentum is fully transferred to the object, the drag force exerted on the disks by ram pressure becomes proportional to the density of the fluid medium in which the galaxy is moving and the square of the relative bulk velocity, which in rich clusters can reach peak values at the pericentre $\gtrsim 1000$ km s^{-1}. In addition, subsequent observations in X-rays (by e.g. Jones and Forman 1984) showed that the gas densities ($\gtrsim 10^{-3}$ cm^{-3}) and temperatures ($\gtrsim$ several keV) in the central regions of such objects are high enough for this and other gas-removal mechanisms (e.g laminar/turbulent stripping, thermal evaporation, starvation, etc.) to be effective.

The idea that the cluster environment plays a key roll on the transformation of spirals into lenticulars is supported by several pieces of observational evidence. One of the most relevant is the morphology-density relation in rich clusters found by Dressler (1980), who convincingly demonstrated that in such systems the fraction of lenticulars rises with local projected density at the same pace that the spiral plus irregular fraction decreases as Fig. 1 (a) well shows. If this segregation had an innate origin then, the phase mixing accompanying the violent relaxation of these large-scale structures would have not preserved the mapping of the initial overdensity to the final density, erasing it. The fact that it is clearly observed in dynamically relaxed galaxy aggregations indicates that the morphology-density relation is (re)built by environmental

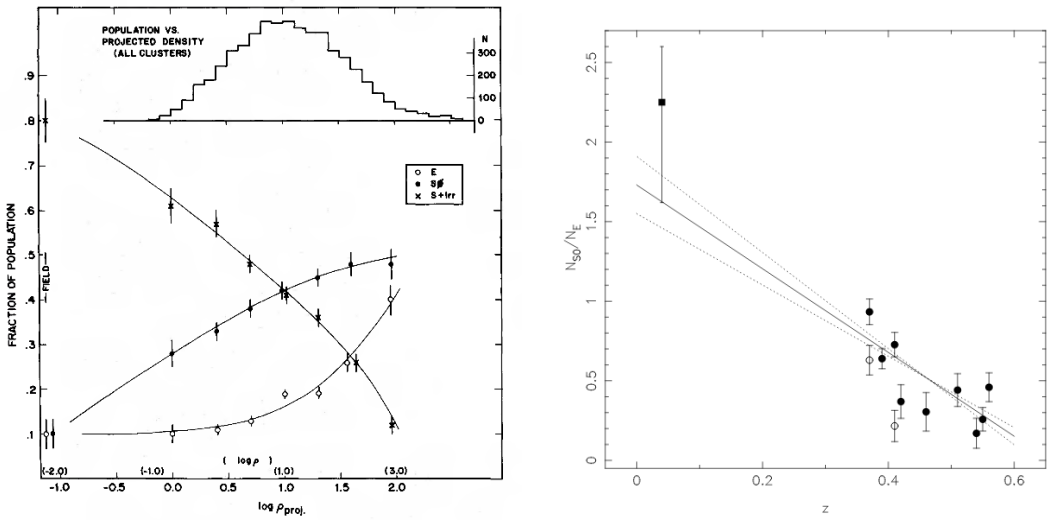

(a) (b)

Figure 1: (a) Original plot from the work of Dressler (1980) which clearly illustrates the morphology-density relation. It shows the fraction of population as a function of the log of the projected density in galaxies Mpc^{-2} for 55 galaxy clusters. (b) The S0/E fraction for clusters in the sample studied by Dressler et al. (1997) as a function of redshift.

mechanisms after clusters form — perhaps after preprocessing has created it at an earlier group stage (Mihos 2004). Yet the most direct evidence that spiral galaxies evolve to become lenticulars is what is generically known as the Butcher-Oemler effect (Butcher and Oemler 1978) consisting in the observation that a number of moderately high-redshift ($z \sim 0.4 - 0.5$) clusters contain a higher proportion of blue, star-forming objects, as well as a factor two lower S0/E fractions than local galaxy aggregations (Dressler et al. 1997; Poggianti et al. 1999; see Fig. 1 (b)).

In spite of being the dominant constituent in the central regions of many rich clusters of galaxies, lenticular galaxies also can be found, albeit rather less frequently[1], in the general field, where hydrodynamical interactions between the interstellar gas of disks and a dense intergalactic medium cannot account for their formation. Explaining the presence of gasless bulge-enhanced galaxies in low density environments requires instead invoking gravitational interactions in the form of close tidal encounters and/or major/minor (dry) mergers (Barnes 1999), since this sort of transformation mechanisms are most effective when the relative speeds of galaxies are similar to their internal stellar velocity dispersions.

We are therefore confronted with the possibility that the S0 galaxies inhabiting the nearby universe actually follow two distinct formation pathways: one part may proceed from evolved spiral galaxies whose gas has been stripped by interactions with either the hot cluster gas or other galaxies, whereas the other, much like elliptical galaxies, may be essentially the result of the gradual (hierarchical) merger of smaller galaxies. Perhaps the best way to settle this question is with the help of observations. The main goal of this present work is precisely to find out whether S0 retain some memory of their past by looking for systematic differences between the typical spectra of these objects as a function of the environment.

[1] In terms of the population fractions, but not necessarily in terms of global numbers. (see Fig. 1 (a))

This approach to the understanding of the origin of the lenticular population is completely new, since past studies have focused essentially on analysing the properties of these objects from photometric data, using either the luminosity functions in near-IR bands (Burstein et al. 2005), the bulge luminosities (Solanes et al. 1989) or the Tully-Fisher relation (Bedregal et al. 2006). The fact that these investigations have often reached contradictory conclusions suggests that such differences, in case they do exist at all, have to be rather subtle. Thus, we expect that the wealth of information that is revealed when the light of an object is divided into its component wavelengths can provide us new and useful insights regarding the processes that shape lenticulars. Statistical spectroscopic studies of galaxies like the one we aim to carry on here have been traditionally limited by the lack of large, systematic extragalactic spectroscopic surveys. This situation, however, has changed recently thanks to the advent of multi-object spectrographs (MOS), that allow multiple galaxies to be observed in each exposure. The primary example is perhaps the Sloan Digital Sky Survey (SDSS; Blanton et al. 2003), which over the last sixteen years has uniformly surveyed more than a quarter of the entire sky providing photometric (u, g, r, i, and z bands) and spectroscopic data for nearly one million galaxies in the nearby universe ($z \lesssim 0.25$).

Using this valuable data mine, we have developed a set of Python scripts, specially written for this project, which compare the composite spectra of different subsets of lenticular galaxies in low- and high-density regions to search for clues as to which evolutionary channel(s) these galaxies have followed. The morphological classifications we use in order to build the S0 subsets proceed from two sources: the detailed visual classification of $\sim 14,000$ galaxies by Nair and Abraham (2010) and from the recently released automatic classification of $\sim 670,000$ galaxies by Domínguez Sánchez et al. (2018) which probably is the largest sample of this kind obtained to date.

The layout of this paper is as follows. In Section II, we address the estimation of local densities for galaxies in several volume-limited sub-samples. Section III is devoted to explain the spectral stacking technique. We apply the whole process to study the S0 population in the two morphological catalogues in Section IV. Finally, in Section V, we summarize the main highlights of this work and we present the forthcoming steps we will take on this research.

II. CALCULATION OF LOCAL DENSITIES

In this calculation we use a sample of clean photometric data[2] (equatorial coordinates, spectroscopic redshifts, r-band apparent magnitudes and Galactic extinctions) from all the galaxies up to $z = 0.108$ in the northern galactic hemisphere of the SDSS Data Release 12 (DR12).

To estimate the local density of a given target galaxy, j, we use the Bayesian density estimator from Cowan and Željko Ivezić (2008), with a correction accounting for the Galactic extinction (Solanes et al. 1996) since it is required owing to the vast extension of the sample in the sky,

$$\mu^{\mathrm{c}}_{2\mathrm{k},j} \propto (10^{0.6\Delta m_j}) \cdot \left[\sum_{i=0}^{k} d_i^2\right]^{-1} \tag{1}$$

where Δm_j is the extinction in apparent magnitude on the r-band affecting the target and d_i is the projected distance to object i among those that have a recessional velocity within 1000 km s^{-1} from the target galaxy. We take the five nearest neighbours, so $k = 5$, with index

[2] Following the criteria of SDSS about clean photometric data. See: `www.sdss.org/dr12/algorithms/photo_flags_recommend/`

$i = 0$ corresponding to the target itself. Notice that in our estimator we write a "proportional to" between the two parts of equation (1) as we are only interested in rating the local density, not in giving a realistic value. However, it is enough for our purpose to distinguishing between low- and high-density environments that we will define from the two extreme quartiles (Q_1 and Q_4) of the local density log-normal distribution function which we use to sort all the galaxies according to the percentile they occupy within a certain volume-limited (see Section II C).

On our calculations of local densities we noticed that although it is quite common to find scientific works in which the depth in the recessional velocity with respect to the target is set to 500 km s^{-1}, we found that sometimes this resulted into almost empty shells where the nearest neighbour was really far from the target, so thinner shells actually led to a less local density estimate.

A. Avoiding edge effects

To apply the procedure just delineated above for each galaxy in the sample leads to an underestimate of the local density for those objects near the edges of the survey. Once the local density of each galaxy has been determined, a simple solution is to remove from our sample all those galaxies whose local density could have been affected by this problematic. The galaxies we eventually discard are those placed at a distance less than $3\sigma_{d_5}$ from the edge, where σ_{d_5} is the scale of the probability density function of the projected distance to the fifth nearest neighbour (see Fig. 2).

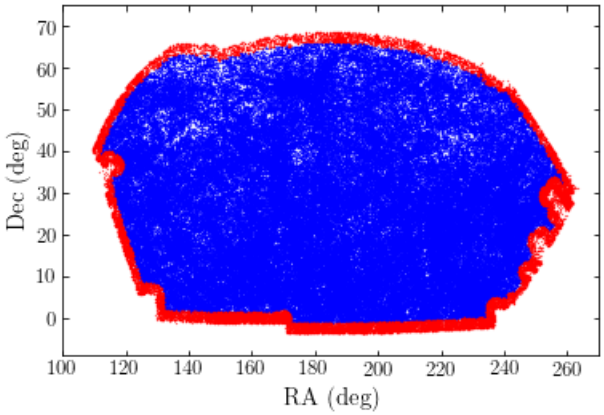

Figure 2: Sky distribution of the objects in the sample. In red, the galaxies under the edge effect, and in blue, those whose local density is well determined.

B. Local density estimator in a flux-limited sample

As happens with most surveys, the SDSS main spectroscopic galaxy sample is flux-limited with an r-band apparent magnitude limit of $m_r = 17.77$ mag (Strauss et al. 2002). Therefore, to avoid the Malmquist bias on our local density estimate, we must cut the sample in the radial coordinate and work with volume-limited sub-sets (VLS), ensuring a minimum absolute magnitude detectable along the full range in redshift delimiting each volume.

For this reason, we calculate r-band absolute magnitudes approximating radial distances by $d \approx cz/H_0$, with $H_0 = 70$ km s^{-1} Mpc^{-1}, and we divide the sample into 6 volume-limited subsets in steps of 0.5 mag, from $(-18.0,\ 0.03)$ to $(-20.5,\ 0.105)$, in which we will estimate the local densities as explained at the beginning of this section. To avoid edge effects, this time along the

line of sight, we increase the volume of each sub-sample in 1000 km s^{-1} in the two extremes of the radial coordinate. Since all our galaxies are nearby ($z \lesssim 0.1$) there is no need to introduce relativistic terms nor $K-$corrections in our calculations. From now on, we will refer to a given VLS by its limits ($M_r,\ z$).

C. Maximisation of sample size

We are interested in comparing the spectral properties of S0 galaxies in low- and high-density environments where this morphological class is represented by unequal fractions. Moreover, the lenticular population only constitutes a $\sim$ 20% of the nearby galaxies. Hence, the number of galaxies involved in our study might play a critical role, specially for those lenticulars belonging to Q_1, which only constitute the 8% of this population (van den Bergh 2009).

Studies pursuing realistic local densities have to restrict the calculation to a single VLS at the expense of a considerable loss of valuable data. However, let us stress that the best estimation for the local density of a target galaxy results from doing the calculation inside the volume delimited in the radial coordinate by the target itself. When working with a flux-limited sample, this is the deepest volume in absolute magnitude at which one can observe the given galaxy and, hence, it includes the maximum number of visible objects near the target yielding, indeed, a better local density estimation. Our method of ranking local densities in percentiles allows us to use more than one sub-sample so we can increase drastically the number of useful targets for our analysis.

Instead of finding the percentile for each galaxy within its optimal volume though (this would entail a huge computational cost since we would have to perform the calculation for as many VLS as galaxies are in the sample), we decide to work with the already mentioned, 6 VLS (see Fig. 3). We proceed with the local density estimation of every galaxy inside each of these VLS, rating each object according to the percentiles they occupy in the local density distribution function of each volume-limited, creating a catalogue of galaxies in the SDSS DR12 with our own ranking in local density as follows:

1. The local density of all the galaxies inside the smallest VLS, i.e., ($-18.0,\ 0.033$), are calculated. This yields a log-normal probability density function which is used to sort the galaxies according to the percentiles. We add this information to our local density catalogue.

2. We proceed with the next VLS, ($-18.5,\ 0.042$), rating by the percentiles the galaxies therein. This time, though, we only add to our local density catalogue those new galaxies, with $M_r < -18.5$ and $0.033 < z \leq 0.042$, that were not inside the previous VLS.

3. Likewise, we perform this classification, sub-sample by sub-sample, until we almost cover the whole SDSS DR12 main spectroscopic galaxy sample up to $z \sim 0.1$.

After this process, those galaxies in percentiles below the 25% (i.e., in Q_1) are considered to be at low-density environments. Those in percentiles above the 75% (i.e., in Q_4) are considered to be at high-density environments. The result produced by our classification is illustrated by wedge diagrams in Fig. 4. Bear in mind, however, that this procedure is only valid to distinguish the kind of environment according to the local density but does not allow to work with realistic local density values and must never substitute the exclusive use of a single volume-limited for those situations requiring it.

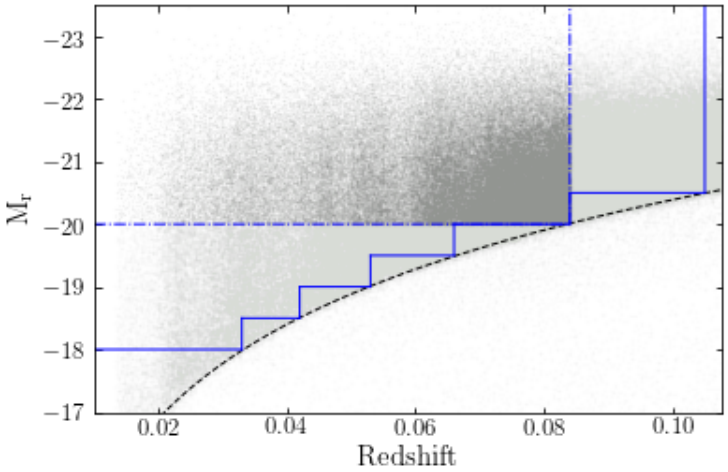

Figure 3: Scatter plot of galaxy absolute magnitude in the r-band as a function of redshift. The black dashed line shows the faint-end limit of the SDSS main spectroscopic galaxy sample at $m_r = 17.77$ mag. The light grey represents objects in the main sample. In dark grey and delimited by a dot-dashed blue line, the sub-sample of galaxies containing most S0 galaxies from the two catalogues we will use (see Section IV A). The solid blue line exemplifies the increase in the number of galaxies resulting from extending the study towards 6 VLS.

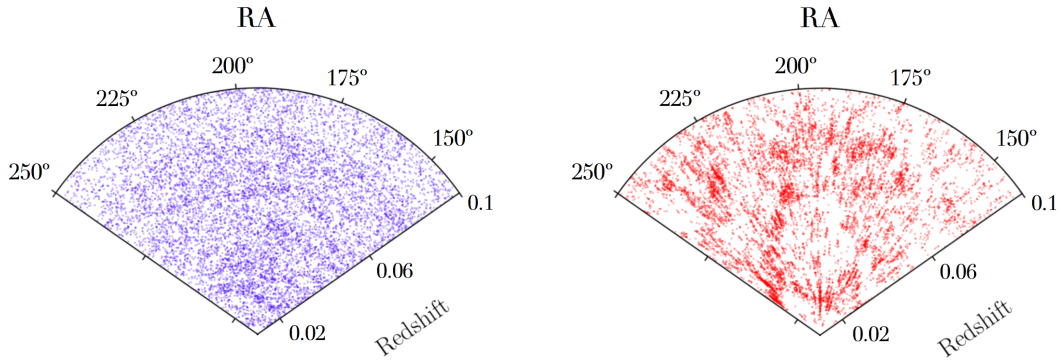

(a) (b)

Figure 4: Wedge diagrams obtained from ranking the galaxies inside the 6 VLS according to their percentiles from the local density distribution function. (a) shows how galaxies belonging to Q_1 (i.e., to low-density environments) distribute homogeneously while in (b), some structure is observed for the galaxies in Q_4 (i.e., in high-density environments). To avoid overcrowding in both diagrams, we only show a fraction of the whole sub-sample.

III. BUILDING COMPOSITE SPECTRA

This section is devoted to explain the stacking technique, which is, perhaps, the core of this work. It is based on the algorithm described in detail in Mas-Ribas et al. (2017), to which we have introduced some modifications to adapt it to our purposes.

The process starts shifting each spectrum to the laboratory rest-frame. Since the spectra are binned with constant logarithmic dispersion[3], this correction is given by $\log \lambda_r = \log \lambda_o - \log(1+z)$, where λ_r is the rest-frame wavelength and λ_o is the observed wavelength. The flux and its error are re-binned by interpolation into pixels of constant $\log \Delta\lambda = 0.0001$, so the resolution of the original spectra is preserved along the full visible range. Examining the mask, we remove from the analysis any problematic pixel[4].

In order to properly compare fluxes of galaxies which are at different distances, a normalization factor with respect to an arbitrary value considered the continuum is assigned to each spectrum. The selection of this continuum must be done a priori, observing a reduced sample of the studied objects, looking for smooth wavelengths ranges free of emission or absorption lines. We take the following wavelength intervals from Dobos et al. (2012), $(4200-4300,\ 4600-4800,\ 5400-5500\ \&\ 5600-5800)$ Å. This factor is given by the following expression

$$n_j = \sum_i \frac{f_{ij}}{N_j} \tag{2}$$

where f_{ij} is the flux in pixel i of the spectrum j and the sum runs over the N_j pixels in the four intervals conforming the continuum. Those spectra with more than a 20% of bad pixels within the normalization ranges are discarded. Then, the signal-to-noise ratio (S/N) computed for the same four wavelength ranges is used to assign a weight to each spectrum,

$$s_j = \frac{\sum_i f_{ij}/N_j}{\left(\sum_i e_{ij}^2/N_j\right)^{1/2}} \tag{3}$$

with e_{ij} the error linked to f_{ij}. Once all the spectra have these two quantities determined, they are stacked together yielding the mean flux as a weighted average over all the spectra:

$$\bar{f}_i = \frac{\sum_j s_j (f_{ij}/n_j)}{\sum_j s_j} \tag{4}$$

where $\bar{f}_i$ is the mean flux of the pixel i. The error we assign to the mean flux is the sample standard deviation with respect to the composite spectrum at each pixel:

$$\sigma_{\bar{f}_i} = \sqrt{\frac{\sum_j \left((f_{ij}/n_j) - \bar{f}_i\right)^2 s_j}{\sum_j s_j}} \tag{5}$$

Finally, we remove the outliers with a 3σ-clipping algorithm which evaluates how much a spectrum deviates from the mean. For each spectrum, it finds the average of the differences between the flux at each pixel with respect to the mean flux. Next, it builds the distribution function of the averaged differences from all the spectra and discards those that deviate more than 3σ from the mean of the distribution which is assumed to be 0. The process repeats until convergence.

---

[3] For more information about SDSS optical data, visit: `http://www.sdss.org/dr12/spectro/spectro_basics/`
[4] Description of each flag: `http://www.sdss.org/dr12/algorithms/bitmasks/#SPPIXMASK`.

IV. STUDY OF THE LENTICULAR POPULATION

Here we present the comparison of the composite spectra characterizing the lenticular population at low- and high-density environments. The results are shown in Fig. 5 and 6, separately, for two different S0 samples which we will introduce in Subsection IV A. Even though lenticular galaxies are popularly known to be gas deficient, we also investigate the possible impact of including edge-on S0 galaxies on the stacked spectra as a function of the kind of environment (Figs. 7, 8, 9 and 10), studying if the mean spectra depend on the inclination angle of the galaxies in the sample. Finally, in Figs. 11 and 12, we show the results from the first approach to a qualitative study of the spectral classification as a function of the local density and inclination.

A. Galaxy samples

The first catalogue we will use to study the S0 population is the visual morphological classification of 14,034 galaxies by Nair and Abraham (2010) (NA10 hereafter). It has been a reference for several works since it is one of the largest visual classification ever performed, including as well many photometric and physical parameters. They identify the T-Type number, based on the Carnegie Atlas of Galaxies (Sandage and Bedke 1994), of their sample of galaxies in the SDSS Data Release 4. The T-Type they use goes along the Hubble sequence, from -5 for ellipticals to 10 for irregular types, where S0 range from -3 to 0.

The other catalogue we will work with is an automatic classification of $\sim 670,000$ galaxies in the SDSS Data Release 7 by Domínguez Sánchez et al. (2018) (DS18 hereafter). The authors obtained the classification through Deep Learning algorithms using Convolutional Neural Networks. Using the Galaxy Zoo 2 (Willett et al. 2013) and Nair and Abraham catalogue to train the neural networks, they assign a T-Type to their sample, but also, they provide a probability of being S0 (P_{S0}) to each target. This allows to better distinguish between ellipticals and lenticulars. Under these considerations, in this current work any object with T-Type ≤ 0 and $P_{S0} > 0.9$ is assumed to be a lenticular galaxy. We set the arbitrary value for the probability trying to maximise the number of S0 while preserving the purity of the sample as far as possible.

The result of cross-matching these two catalogues with ours in local density, appears summarized in Table I. Note how for DS18 the number of S0 is almost doubled after applying our procedure of ranking the local densities along 6 volumes in contrast to limiting the analysis to a single VLS.

Table I: Volume-limited sub-sets with the total number of galaxies, number of S0 galaxies added by each VLS to the whole sample and to Q_1 and Q_4 for each catalogue. Last two rows show, respectively, the sum over each sub-set and the numbers for the VLS richest in S0 galaxies.

$(M_r,\ z)$	N	N10			DS18		
		Δ S0 VLS	Δ S0 Q_1	Δ S0 Q_4	Δ S0 VLS	Δ S0 Q_1	Δ S0 Q_4
$(-18.0,\ 0.033)$	19837	641	156	188	1149	246	374
$(-18.5,\ 0.042)$	31631	279	76	60	1187	224	420
$(-19.0,\ 0.053)$	48933	270	61	55	2073	482	634
$(-19.5,\ 0.066)$	74386	200	39	60	3943	852	1253
$(-20.0,\ 0.084)$	117250	84	16	27	7698	1692	2263
$(-20.5,\ 0.105)$	140529	10	1	5	7619	2144	1935
TOTAL		**1484**	**349**	**395**	**23669**	**5640**	**6879**
ONLY $(-20.0,\ 0.084)$		**1395**	**320**	**375**	**12479**	**2732**	**3718**

B. Low- vs. high-density environments

In Fig. 5 we present the composite spectra of lenticular galaxies from the sample NA10 at low- and high-density environments. For the lenticulars in the field (blue line) it can be observed an enhancement on the main emission lines as well as a bluer continuum with respect to their counterparts placed at high density environments (red line). When statistics are increased using the sample DS18, these differences become even more obvious as it is shown in Fig. 6.

Although scarce, in some cases S0 galaxies do have star formation activity as the presence of Hα Balmer emission ($\lambda = 6562.8$ Å) proves, since it is the most direct indicator of the current ($< 4 \times 10^6$ yrs) massive ($> 8M_\odot$) star formation activity in galaxies (Kennicutt 1998). The emission lines are caused by clouds of ionized gas where giant stars of the types O and B are born. However, the atmospheres of those giant stars contribute to the Balmer series in absorption, yielding a dilution of the hydrogen emission lines which grows in importance towards the higher order Balmer lines: while Hβ emission ($\lambda = 4862.7$ Å) is moderately affected by the absorption, all of the Hδ emission (4102.9 Å) is usually lost into the absorption (Olofsson 1995).

After the stacking, we observe that this phenomenon affects much less to the S0 in Q_1 than those in Q_4 and that the differences intensify when we increase the statistics with the sample DS18. This feature is indicating that lenticulars in the field do have enough reservoir of ionized gas and young massive blue stars (in relative terms) to, at least, give rise to the Balmer emissions and a slightly bluer continuum in comparison with the lenticulars in high density regions. Nevertheless, these result is not enough to distinguish whether these features are intrinsic from the kind of environment where the S0 are found or whether they are a signature of the evolution undergone by the galaxy.

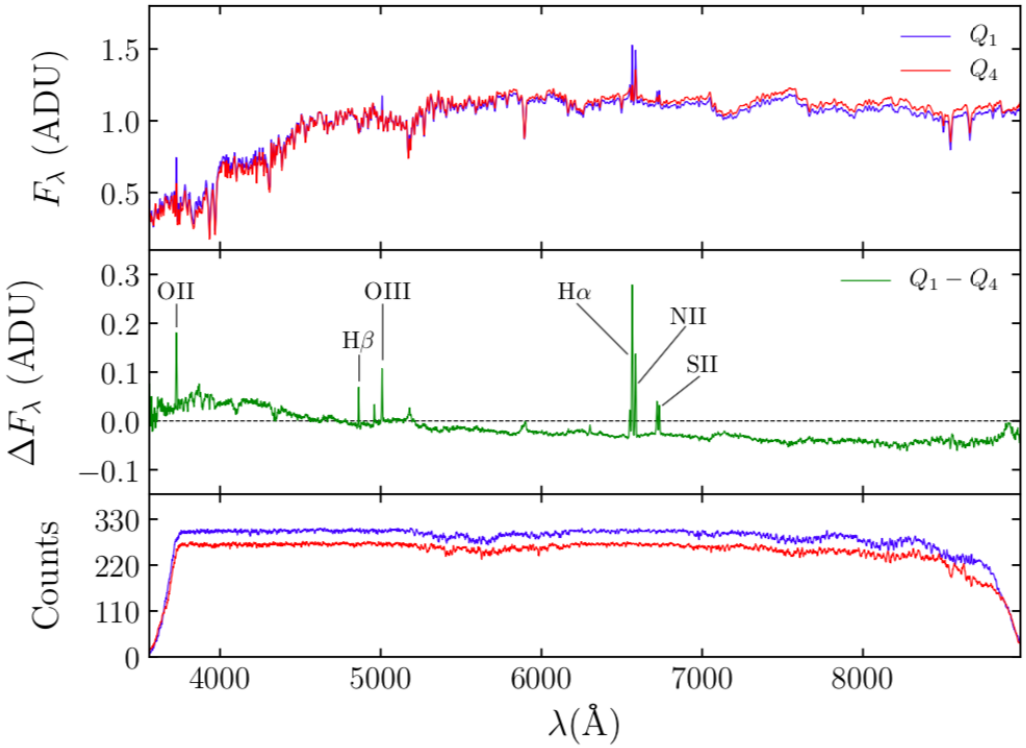

Figure 5: First panel shows the comparison between the mean flux of S0 galaxies from NA10 at low- (blue line) and high- (red line) density environments. The green line on the middle panel corresponds to the subtraction $\Delta F_\lambda = F_\lambda^{Q_1} - F_\lambda^{Q_4}$. A label has been added to indicate some of the main emission lines identified in Table A1. The bottom panel shows the number of stacked spectra used to compute the mean flux at each pixel with the same colour code as the first panel.

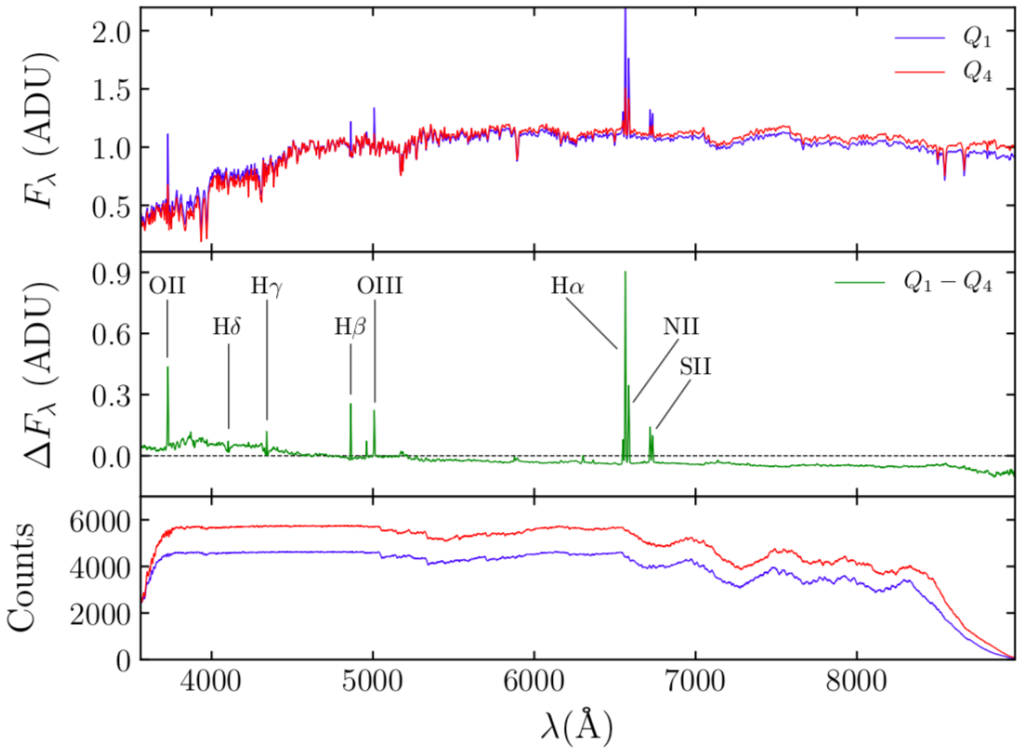

Figure 6: Similar comparison as in Fig. 5, but for the DS18 galaxy sample (see Table A1).

C. Edge-on vs. face-on

Using the axis ratio b/a from two-dimensional, single-component Sersic fit in the r-band provided by the NASA-Sloan Atlas we divide the sub-sets depending on the galaxy inclinations, $i = \arccos(b/a)$, in face-on ($i < 60^o$) and edge-on ($i \geq 60^o$) where b and a are the minor and major axis from the Sersic fit. To evaluate the extinction, we subtract the mean flux of the edge-on from the mean flux of the face-on lenticulars for each of the sub-sets in Q_1 and Q_4. The results are shown for the two galaxy samples in Fig. 7 and Fig. 8 for NA10, and in Fig. 9 and Fig. 10 for DS18.

In both environments, as continuums indicate, face-on lenticulars are bluer and also have stronger emission lines than edge-on lenticulars, although these differences are notably greater in the field and for the DS18 lenticular sample. Specially, it stands out that for the sample of lenticulars from DS18 at high-local densities (Fig. 10), the differences are quite larger than those one may expect to find in these kind of populated environments, where classical lenticulars are expected to have virtually null amount of gas. Contrarily, the typical behavior of the composite spectra of S0 in the configurations here studied, would be more similar to what is observed in Fig. 8, where both, main lines and continuum, seldom vary from one configuration to the other. These result suggest that the sample of lenticulars from DS18 could be contaminated by dusty spiral galaxies of the Type Sa which are capable, even at high-density regions, to retain a significant amount of gas and dust which contributes to a certain extinction of the light when they are observed edge-on.

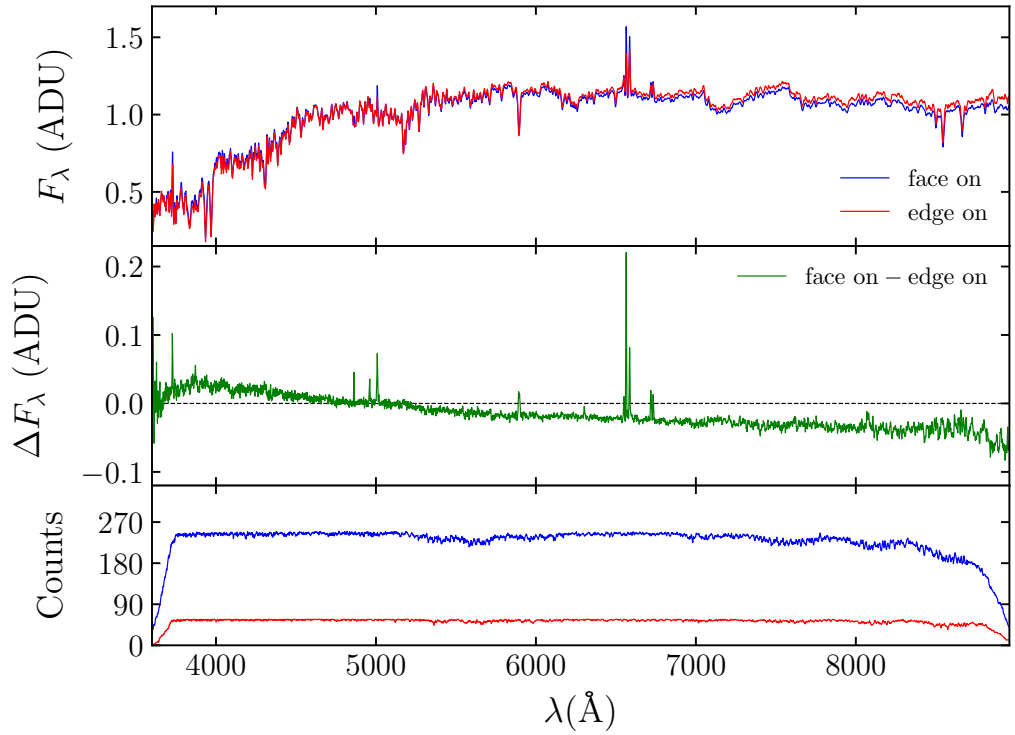

Figure 7: Same as Fig. 5, but for the composite spectra of face-on (blue line) and edge-on (red line) S0 in NA10 at low local densities, (i.e., Q_1). The green line in the middle panel difference between the mean flux from face-on lenticulars and the mean flux from edge-on lenticulars, i.e., $\Delta F_\lambda = F_\lambda^{face-on} - F_\lambda^{edge-on}$.

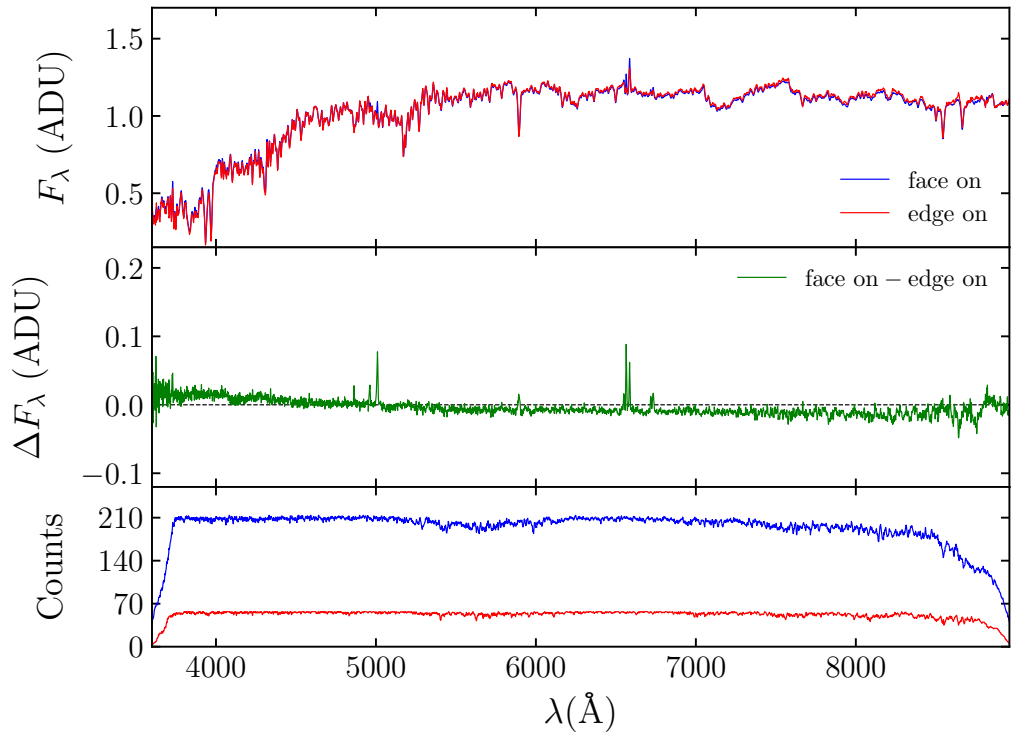

Figure 8: Same as in Fig. 7 but showing the comparison between the composite spectra of face-on and edge-on S0 galaxies at high local densities, (i.e., Q_4) from the sample NA10.

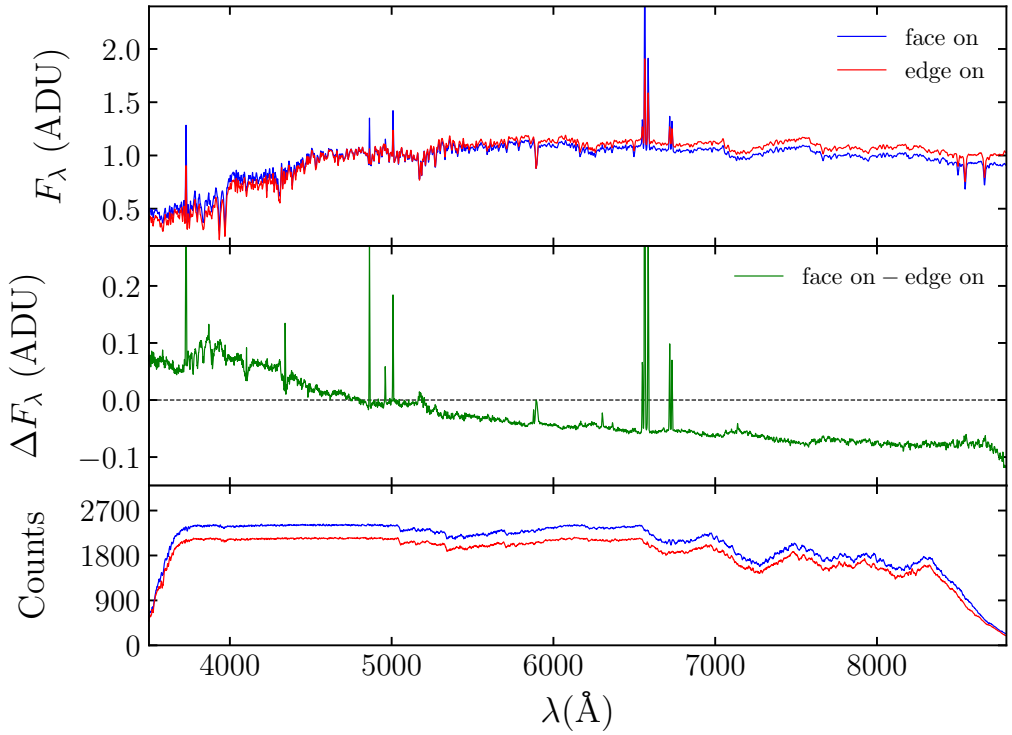

Figure 9: Same as in Fig. 7, but showing the comparison between the composite spectra of face-on and edge-on S0 galaxies in Q_1 from the sample DS18.

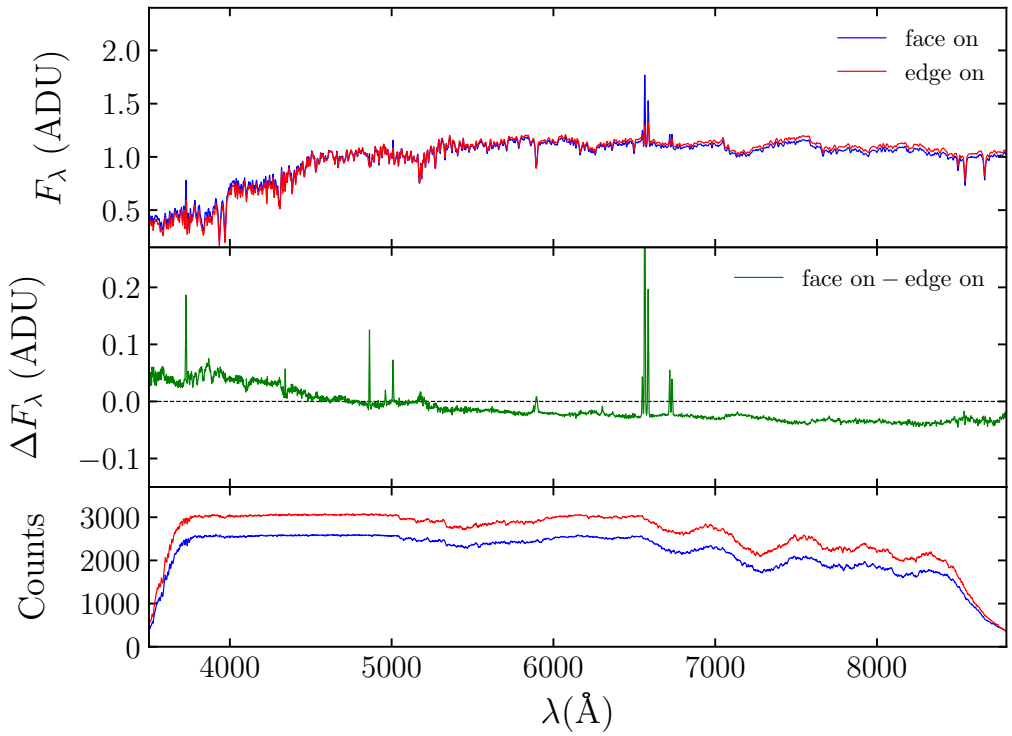

Figure 10: Same as in Fig. 7, but showing the comparison between the composite spectra of face-on and edge-on S0 galaxies in Q_4 from the sample DS18.

D. Spectral vs. morphological classification

In addition, owing to the finds above mentioned (Section IV C) suggesting a possible contamination, we have studied qualitatively the dispersion in the spectroscopic samples, contrasting it with the work of Sánchez Almeida et al. (2011), who compared typical morphological classifications (among them the catalogue we are studying from Nair and Abraham) with his Automatic Spectroscopic K-means (ASK) based classification quantifying the spectral dispersion once morphology is fixed. They found that for the S0, the ASK varies with a standard deviation between 3 and 4 spectral classes, being this, one of the most scattered population. After all, they concluded that this scatter is not produced by problems in the classification but is intrinsic of each Hubble type and it is not reduced when particular sub-sets, such as low- and high-density environments or face-on galaxies, are considered.

Our results shown in Fig. 11 (left column) are indicating, however, that there exists a dispersion among the spectral samples of S0 galaxies (before applying the 3σ-clipping) from both catalogues, which seems subtly wider for those galaxies from NA10 at low-density environments. As can be seen in Fig. 11 (right column), this issue does not compromise our composite spectra since our clipping successfully discards the outliers. Nevertheless, it casts some doubts on the purity of the samples but also about the S0 class itself: Are the morphological classifications that we are studying reliable? Should the answer be affirmative, then how wide is the family of lenticulars in the field and why such dispersion is not as large for the population in high density environments?

Interestingly, we find as well that the dispersion on the spectroscopic sample is reduced when only edge-on S0 galaxies from the catalogue of Nair and Abraham are considered for both kinds of environments, contrary to what happens with the sample of Domínguez Sánchez et al., which, indeed, presents a similar dispersion in the face-on than in the edge-on sub-sets (see Fig. 12).

Although we do not show any plot in this present work, let us finish explaining how we investigate this second scatter, only present among one of the face-on S0 samples. We repeat the stacking for both catalogues, but now, splitting each face-on sample in two sub-groups in inclination: "completely" face-on ($0^o \leq i < 30^o$) and "half-way" between face-on and edge-on ($30^o < i \leq 60^o$). For the NA10 S0 samples and in both environments, the results show how the scatter disappears when only completely face-on lenticulars are considered, but it reappears in the half-way sub-group. On the other hand, the dispersion remains the same when this analysis is performed with the DS18 S0 samples. We are still working on the interpretation of this last results. Yet they seem to point towards a possible contamination, by other morphological types different from S0 (perhaps E and some Sa), in the face-on NA10 sub-sample.

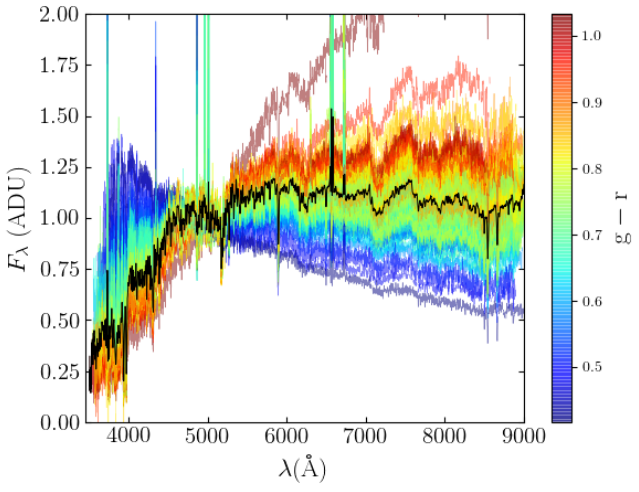

(a) Lenticular galaxies from NA10 in Q_1 before clipping.

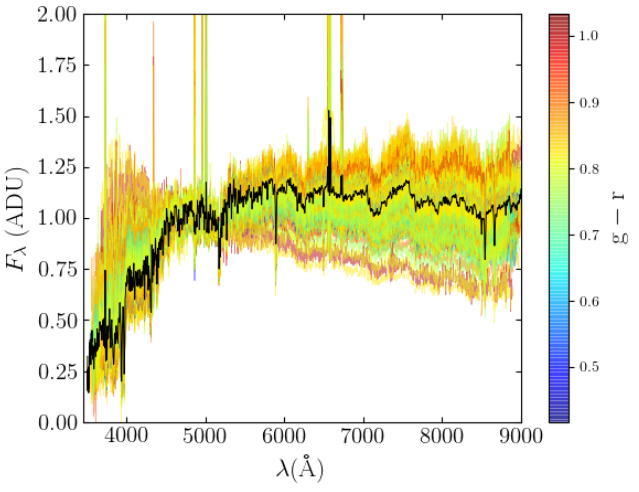

(b) Lenticular galaxies from NA10 in Q_1 after clipping.

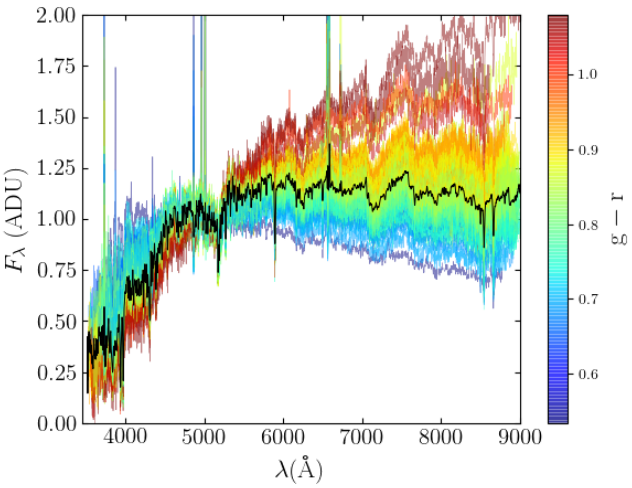

(c) Lenticular galaxies from NA10 in Q_4 before clipping.

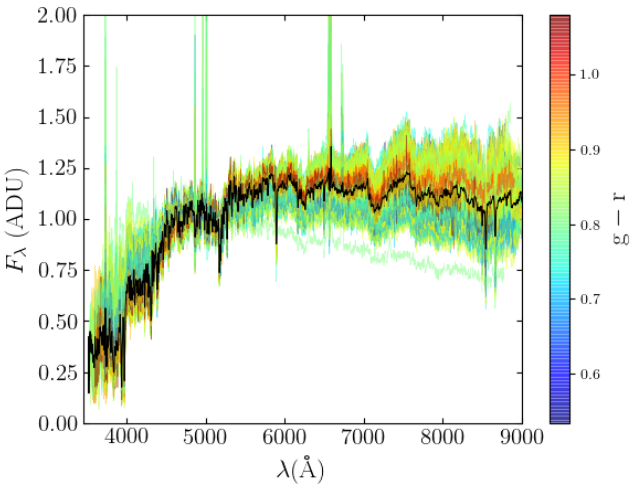

(d) Lenticular galaxies from NA10 in Q_4 after clipping.

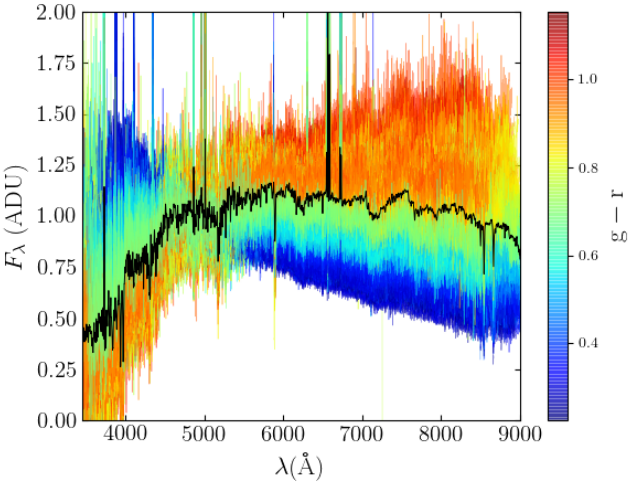

(e) Lenticular galaxies from DS18 in Q_1 before clipping.

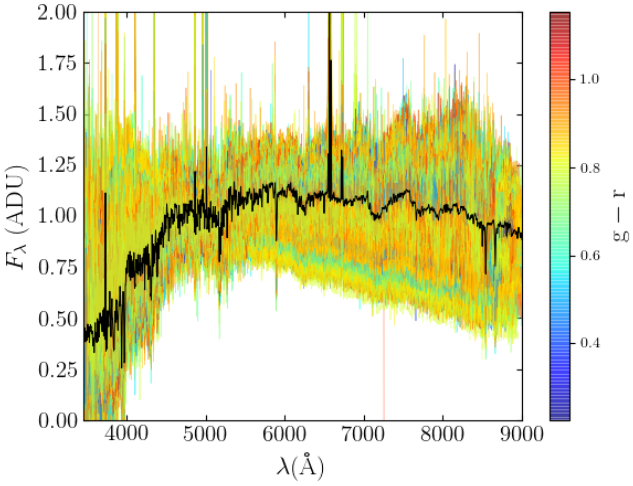

(f) Lenticular galaxies from DS18 in Q_1 after clipping.

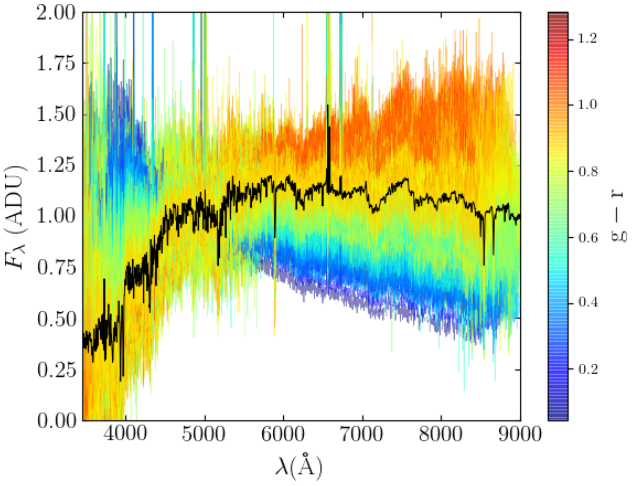

(g) Lenticular galaxies from DS18 in Q_4 before clipping.

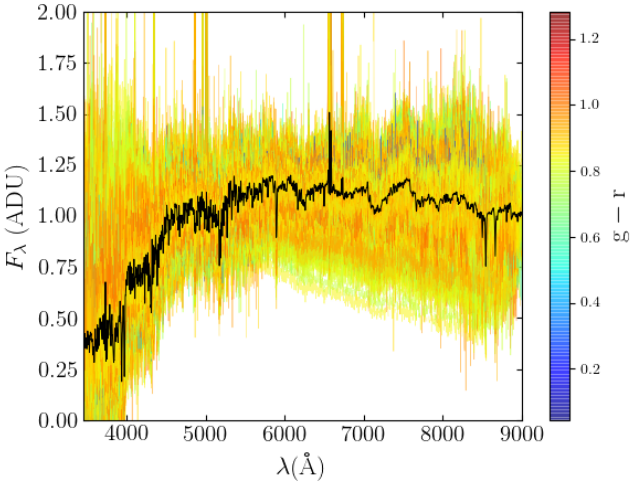

(h) Lenticular galaxies from DS18 in Q_4 after clipping.

Figure 11: Spectral dispersion of each composite spectrum for the two samples of S0 galaxies, from NA10 and DS18. The black line corresponds to the mean flux before (left column) and after (right column) performing the 3σ-clipping. To show the dispersion in each sample we have overlapped all the spectra used in the stacking represented by the $g-r$ colour index. Note the wide range of spectra that are mixed before applying the clipping, specially for lenticulars at low local densities.

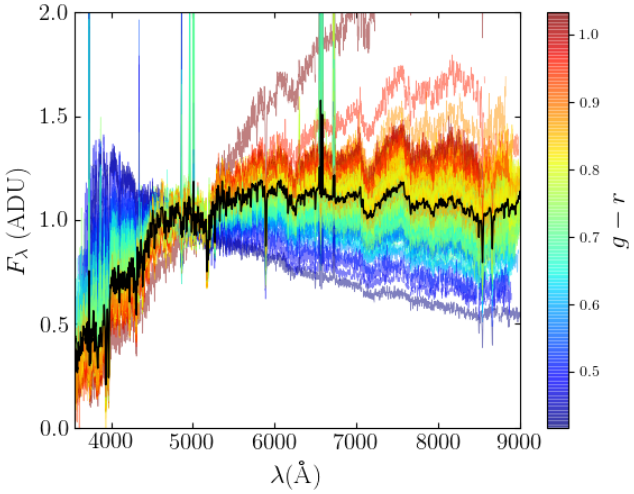

(a) Face-on galaxies from NA10 in Q_1 before clipping.

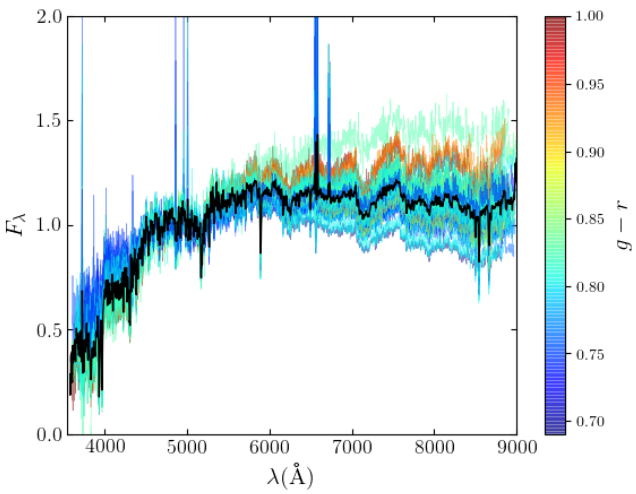

(b) Edge-on galaxies from NA10 in Q_1 before clipping.

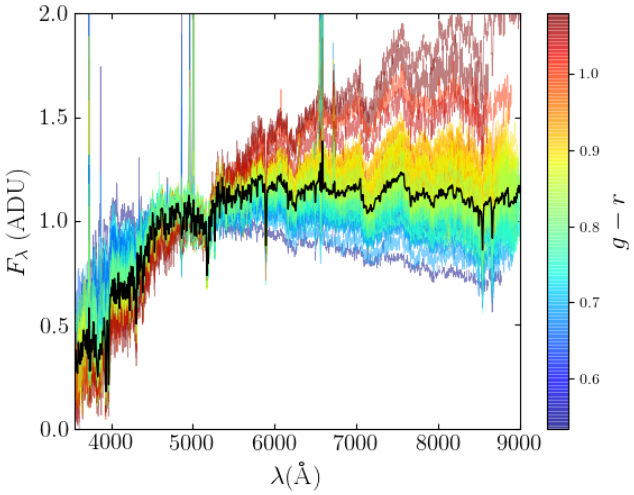

(c) Face-on galaxies from NA10 in Q_4 before clipping.

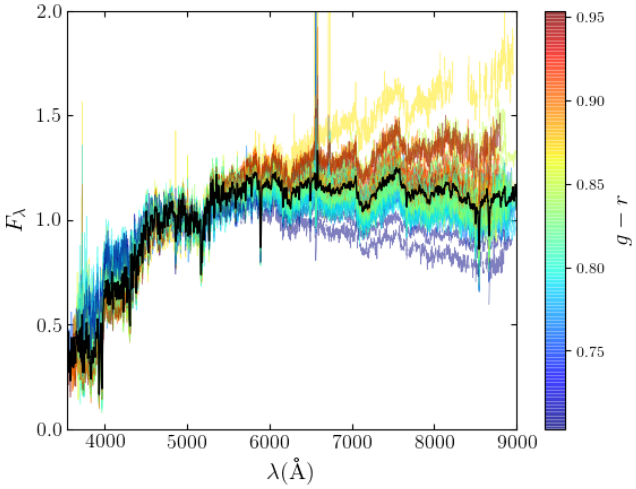

(d) Edge-on galaxies from NA10 in Q_4 before clipping.

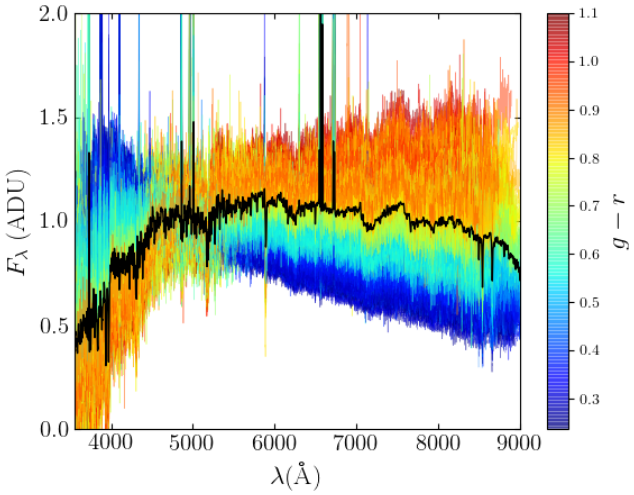

(e) Face-on galaxies from DS18 in Q_1 before clipping.

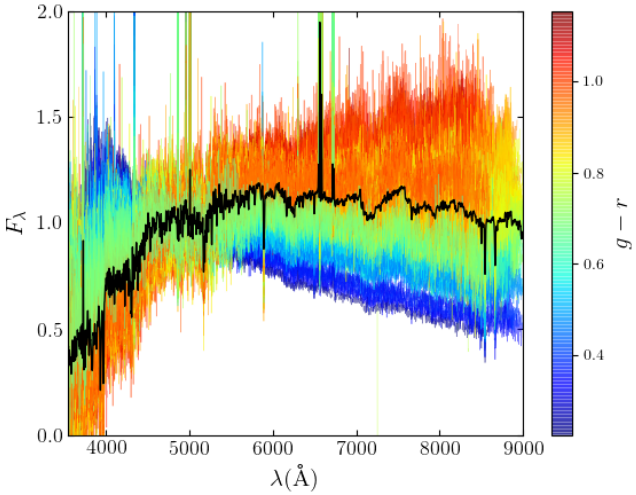

(f) Edge-on galaxies from DS18 in Q_1 before clipping.

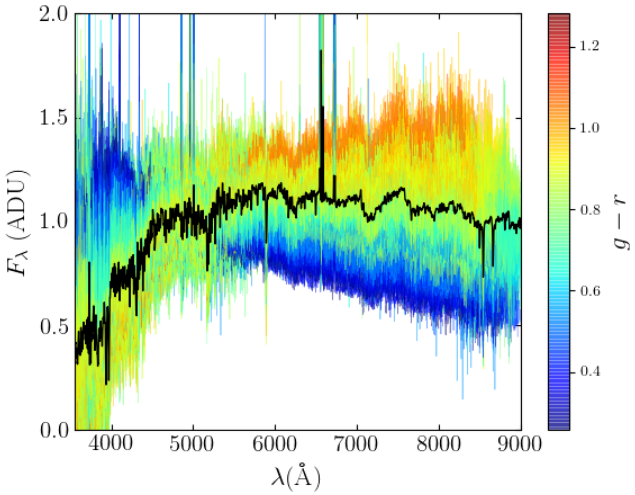

(g) Face-on galaxies from DS18 in Q_4 before clipping.

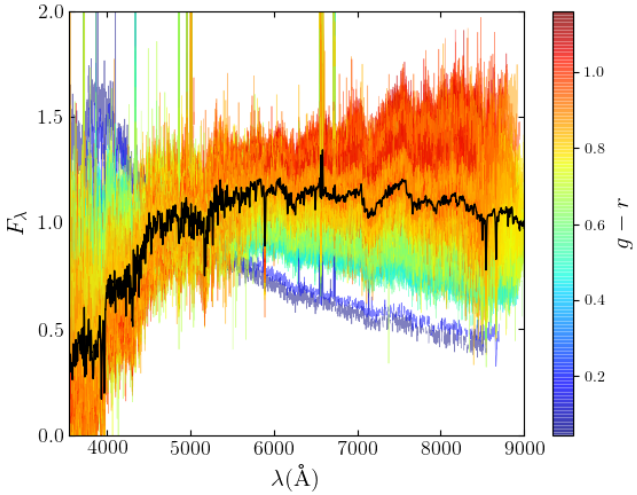

(h) Edge-on galaxies from DS18 in Q_4 before clipping.

Figure 12: Same as Fig. 11 but for face-on (left column) and edge-on (right column) S0 from each sample, NA10 and DS18, before performing the 3σ-clipping. Note how, indistinctly for both kinds of environments, the scatter decreases from face-on to edge-on galaxies for the samples from Nair and Abraham (2010) but it barely changes for the galaxies from Domínguez Sánchez et al. (2018).

V. SUMMARY AND FUTURE WORK

- We have developed a methodology that allows to study the imprint left by the environment on the optical spectrum of galaxies. The method, which is particularly suitable for the new generation of surveys based in MOS spectroscopy that contain a vast quantity of spectral data, requires the calculation of extinction-corrected local 3-dimensional densities in volume-limited subsets of galaxies free of edge effects to sort them according to the percentiles they occupy in the local density distribution function, as well as the creation of high S/N composite spectra after the shifting, re-binning, normalizing, weighting and stacking of the individual spectra of galaxies belonging to a given class.

- The local density classification has been applied to the galaxies in the 6 VLS between $(-18.0,\ z = 0.033)$ and $(-20.5,\ z = 0.105)$ in the SDSS DR12 main spectroscopic galaxy sample, ranking each object by its position in the local density distribution function computed in an optimal VLS for each target. Instead of working with a single volume-limited, to use this technique allows us to increases drastically the number of available objects for the study.

- Our tool has been applied to lenticular galaxies within the SDSS Legacy Volume. First, using a reduced select sample of S0 galaxies identified by the expert "human eye" of Nair and Abraham and then to the huge sample of S0 whose morphology has been determined using deep learning algorithms by Domínguez Sánchez et al.. For both samples we find important differences in the continuum and on the heights of the main emission lines between the composite spectra of S0 galaxies in Q_1 and Q_4. A first qualitative analysis of these differences indicates that lenticulars in low-density environments are bluer and may have a relevant amount of ionized hydrogen and star formation activity, at least in relative terms with respect to their high-density counterparts. The results we find are consistent with those in Kuntschner et al. (2002) and also with the work of Xiao et al. (2016).

- In addition, the results from splitting the lenticular samples in face-on and edge-on supports

the main idea that lenticulars in low-density environments are not as gas deficient as popularly thought, but do have a certain reservoir of gas and/or dust able to cause enough extinction to perceive edge-on galaxies slightly redder than face-on galaxies. Nevertheless, the important change on the continuum in the comparison edge-on vs. face-on arising from the lenticulars from DS18 in Q_4 deviates a bit from the picture we have of a "classical" S0 in a high density environment which is expected to be gas deficient. This should be a warning to revise the morphological classification of the lenticular galaxies in this catalogue before carrying out more analysis.

- What is more, a first visual inspection of the spectral scatter in each sample of S0, but specially for the lenticulars in NA10, suggests that, for this population in the field, there is a slightly wider dispersion than in high-density environments. This feature will be investigated in more detail in the future.

- We have observed as well a wider dispersion for face-on than for edge-on S0 only noticeable in the NA10 sample. We attribute this effect to a possible contamination of the sample owing to the difficulty for the human eye to distinguish, from other types, the projection of an S0 at intermediate inclinations ($30^o < i \leq 60^o$). Seems that machines are "projection-proof" in this sense. Thus, removing edge-on galaxies prevents us from extinction, but face-on S0 galaxies visually classified can introduce a considerable dispersion. Yet the interpretation of these results is pending before we could extract further conclusions.

- At this moment, we are not able yet to claim clear evidences from our results shown in Fig. 5 or Fig. 5, neither against nor in favour, of any of the two formation mechanisms, i.e., ram pressure stripping in clusters nor galaxy mergers in the general field. The difficulty relies now on distinguishing whether these features are intrinsic from the kind of environment where the S0 are placed (e.g. clusters are more efficient removing gas and stopping star formation) or whether they are a signature of the formation pathways (e.g. a recent merger from which a rejuvenated stellar population with blue giant stars, born from the starburst, is the responsible for ionizing the gas giving rise to the enhanced emission lines). However, in this work we have provided some interesting clues which will be used as a starting point for future research.

The following step will be to familiarise and evaluate the goodness of the morphological samples we are using, specially with that from Domínguez Sánchez et al. which is a diamond in the raw that should be further exploited. Still we have to evaluate if our criterion to determine that a given target is placed in a high density environment from the local density estimation is giving us actual cluster members or, on the contrary, members of large but less dense galaxy groups. For this later purpose, we will cross-match our high-density samples with some of the available SDSS cluster catalogues.

We will complete this characterization of the lenticular population in low- and high-density environments with 1-dimensional data extracted from photometric measurements. Also providing the analysis with a more quantitative tone by determining chemical abundances and metallicities as well as quantifying the scatter in the spectral samples. It is pending as well to perform bulge-disk decomposition of our lenticulars to try to constrain the formation paths of these galaxies by seeking signatures of recent galaxy mergers that could be encoded in the spectra from the bulges of those S0 in the field (Charbonnel et al. 2011, Xiao et al. 2016). With this aim, our final goal will be to get to study this population with 3-dimensional data making use of Integral Field Spectroscopy.

Acknowledgments

First of all, I would like to thank Josep Maria Solanes, who has taught me so much and has bet on me from the beginning. Special thanks to Jaime Perea and Ascensión del Olmo from the *Instituto de Astrofísica de Andalucía* (IAA-CSIC) for their advice on the spectral analysis and their critical eye with my results. I would also like to thank the kind people from *la Reial Acadèmia de Ciències i Arts de Barcelona* (RACAB) for their attention and constant encouragement and my mates from the master who have given me good ideas and have helped me in several occasions. Finally, to my family for backing me up unconditionally.

References

Barnes, J. E. (1999). Dynamics of Mergers Remnants. In Barnes, J. E. and Sanders, D. B., editors, *Galaxy Interactions at Low and High Redshift*, volume 186 of *IAU Symposium*, page 137.

Bedregal, A. G., Aragón-Salamanca, A., and Merrifield, M. R. (2006). The tully–fisher relation for s0 galaxies. *Monthly Notices of the Royal Astronomical Society*, 373(3):1125–1140.

Blanton, M. R., Lin, H., Lupton, R. H., Maley, F. M., Young, N., Zehavi, I., and Loveday, J. (2003). An efficient targeting strategy for multiobject spectrograph surveys: the sloan digital sky survey "tiling" algorithm. *The Astronomical Journal*, 125(4):2276.

Burstein, D., Ho, L. C., Huchra, J. P., and Macri, L. M. (2005). The k-band luminosities of galaxies: Do s0s come from spiral galaxies? *The Astrophysical Journal*, 621(1):246.

Butcher, H. and Oemler, Jr., A. (1978). The evolution of galaxies in clusters. I - ISIT photometry of C1 0024+1654 and 3C 295. ApJ, 219:18–30.

Charbonnel, C., Montmerle, T., and Bournaud, F. (2011). Star formation in galaxy interactions and mergers. *European Astronomical Society Publications Series*, 51:107–131.

Cowan, N. B. and Željko Ivezić (2008). The environment of galaxies at low redshift. *The Astrophysical Journal Letters*, 674(1):L13.

Dobos, L., Csabai, I., Yip, C.-W., Budavári, T., Wild, V., and Szalay, A. S. (2012). A high-resolution atlas of composite Sloan Digital Sky Survey galaxy spectra. MNRAS, 420:1217–1238.

Domínguez Sánchez, H., Huertas-Company, M., Bernardi, M., Tuccillo, D., and Fischer, J. (2018). Improving galaxy morphologies for sdss with deep learning. *Monthly Notices of the Royal Astronomical Society*, 476(3):3661–3676.

Dressler, A. (1980). Galaxy morphology in rich clusters - Implications for the formation and evolution of galaxies. ApJ, 236:351–365.

Dressler, A., Oemler, Jr., A., Couch, W. J., Smail, I., Ellis, R. S., Barger, A., Butcher, H., Poggianti, B. M., and Sharples, R. M. (1997). Evolution since z = 0.5 of the Morphology-Density Relation for Clusters of Galaxies. ApJ, 490:577–591.

Gunn, J. E. and Gott, III, J. R. (1972). On the Infall of Matter Into Clusters of Galaxies and Some Effects on Their Evolution. ApJ, 176:1.

Hubble, E. P. (1936). *Realm of the Nebulae.*

Jones, C. and Forman, W. (1984). The structure of clusters of galaxies observed with Einstein. ApJ, 276:38–55.

Kennicutt, Jr., R. C. (1998). Star Formation in Galaxies Along the Hubble Sequence. ARA&A, 36:189–232.

Kuntschner, H., Smith, R. J., Colless, M., Davies, R. L., Kaldare, R., and Vazdekis, A. (2002). Early-type galaxies in low-density environments. *Monthly Notices of the Royal Astronomical Society*, 337(1):172–198.

Mas-Ribas, L., Miralda-Escudé, J., Pérez-Ràfols, I., Arinyo-i-Prats, A., Noterdaeme, P., Petitjean, P., Schneider, D. P., York, D. G., and Ge, J. (2017). The Mean Metal-line Absorption Spectrum of Damped Lyα Systems in BOSS. ApJ, 846:4.

Mihos, J. C. (2004). cluster galaxies. *Clusters of Galaxies: Volume 3, Carnegie Observatories Astrophysics Series: Probes of Cosmological Structure and Galaxy*, 3:277.

Nair, P. B. and Abraham, R. G. (2010). A Catalog of Detailed Visual Morphological Classifications for 14,034 Galaxies in the Sloan Digital Sky Survey. ApJS, 186:427–456.

Olofsson, K. (1995). Synthetic absorption line strengths in star forming regions, and the effects on the helium abundance determination. A&AS, 111:57.

Poggianti, B. M., Smail, I., Dressler, A., Couch, W. J., Barger, A. J., Butcher, H., Ellis, R. S., and Augustus Oemler, J. (1999). The star formation histories of galaxies in distant clusters. *The Astrophysical Journal*, 518(2):576.

Sánchez Almeida, J., Aguerri, J. A. L., Muñoz-Tuñón, C., and Huertas-Company, M. (2011). Relationship between Hubble Type and Spectroscopic Class in Local Galaxies. ApJ, 735:125.

Sandage, A. (1961). *The Hubble atlas of galaxies*, volume 618. Carnegie Institution of Washington Washington, DC.

Sandage, A. and Bedke, J. (1994). *The Carnegie Atlas of Galaxies. Volumes I, II.*

Solanes, J. M., Giovanelli, R., and Haynes, M. P. (1996). The H i Content of Spirals. I. Field Galaxy H i Mass Functions and H i Mass–Optical Size Regressions. ApJ, 461:609.

Solanes, J. M., Salvador-Sole, E., and Sanroma, M. (1989). The luminosity of galactic components and morphological segregation. AJ, 98:798–805.

Spitzer, Jr., L. and Baade, W. (1951). Stellar Populations and Collisions of Galaxies. ApJ, 113:413.

Strauss, M. A., Weinberg, D. H., Lupton, R. H., Narayanan, V. K., Annis, J., Bernardi, M., Blanton, M., Burles, S., Connolly, A. J., Dalcanton, J., Doi, M., Eisenstein, D., Frieman, J. A., Fukugita, M., Gunn, J. E., Željko Ivezić, Kent, S., Kim, R. S. J., Knapp, G. R., Kron, R. G., Munn, J. A., Newberg, H. J., Nichol, R. C., Okamura, S., Quinn, T. R., Richmond, M. W., Schlegel, D. J., Shimasaku, K., SubbaRao, M., Szalay, A. S., Berk, D. V., Vogeley, M. S., Yanny, B., Yasuda, N., York, D. G., and Zehavi, I. (2002). Spectroscopic target selection in the sloan digital sky survey: The main galaxy sample. *The Astronomical Journal*, 124(3):1810.

van den Bergh, S. (2009). Lenticular galaxies and their environments. *The Astrophysical Journal*, 702(2):1502.

Willett, K. W., Lintott, C. J., Bamford, S. P., Masters, K. L., Simmons, B. D., Casteels, K. R. V., Edmondson, E. M., Fortson, L. F., Kaviraj, S., Keel, W. C., Melvin, T., Nichol, R. C., Raddick, M. J., Schawinski, K., Simpson, R. J., Skibba, R. A., Smith, A. M., and Thomas, D. (2013). Galaxy Zoo 2: detailed morphological classifications for 304 122 galaxies from the Sloan Digital Sky Survey. MNRAS, 435:2835–2860.

Xiao, M.-Y., Gu, Q.-S., Chen, Y.-M., and Zhou, L. (2016). The nuclear activities of nearby s0 galaxies. *The Astrophysical Journal*, 831(1):63.

A1. APPENDIX

Table A1: Main spectral lines with the corresponding wavelength identified in the composite spectra of the S0 galaxy sub-sets in low- (Q_1) and high- (Q_4) density environments from the catalogues by Nair and Abraham (third and fourth columns) and by Domínguez Sánchez et al. (fifth and sixth columns). A letter has been added for comparison between the two sub-samples from each catalogue. "E" denotes a higher emission, "e" a lower emission, "A" a deeper absorption and "a" a shallower absorption. Species and wavelengths from: `http://classic.sdss.org/dr6/algorithms/linestable.html`

SPECIES	λ (Å)	S0 from NA10		S0 from DS18	
		Q_1	Q_4	Q_1	Q_4
OII	3729.9	E	e	E	e
K	3934.7	a	A	a	A
H	3969.6	a	A	a	A
Hδ	4102.9	a	A	E	A
G	4305.6	a	A	E	e
Hγ	4341.7	a	A	E	A
OIII	4364.4	E	e	E	e
Hβ	4862.7	E	A	E	e
OIII	4932.6	e	E	e	E
OIII	4960.3	E	e	E	e
OIII	5008.2	E	e	E	e
Na	5895.6	A	a	A	a
OI	6302.1	E	e	E	e
NII	6549.9	E	e	E	e
Hα	6564.6	E	e	E	e
NII	6585.3	E	e	E	e
SII	6718.3	E	e	E	e
SII	6732.7	E	e	E	e
CaII	8500.4	A	a	A	a
CaII	8544.4	A	a	A	a
CaII	8664.5	A	a	A	a